NUMERICAL STUDY OF INLET CROSS-SECTION EFFECT ON OBLIQUE FINNED MICROCHANNEL HEAT SINK

by

Rajendran VINOTH [a*] ***and Duraisamy SENTHIL KUMAR*** [b]

[a] Centre for Energy, Department of Mechanical Engineering,
Sree Vidyanikethan Engineering College, Tirupati, Andhra Pradesh, India
[b] Department of Mechanical Engineering, Sona College of Technology,
Salem, Tamil Nadu, India

Original scientific paper
https://doi.org/10.2298/TSCI161119133V

The current study is focused on the heat transfer and flow characteristics of an oblique finned micro-channel heat sink with different inlet cross-sections. Water and Al_2O_3-water nanofluid with 0.25% volume fraction were used as heat transfer fluids. The oblique finned micro-channel heat sinks of size 48 × 80 mm were designed with three different inlet cross-sections, namely square, semicircle and trapezoidal. The ANSYS FLUENT simulations validated with the aid of an existing experimental work. The flow regime in micro-channel heat sink is constrained to laminar flow in the study. The three inlet cross-sections have been investigated by varying Reynolds number for Water and Al_2O_3-water nanofluid. The trapezoidal cross-section with average heat transfer rate 3.35% and pressure drop 8.6% is more efficient than other cross-sections due to larger wall area and effective entrance length. The oblique finned micro-channel heat sink with the trapezoidal cross-section is suitable for the micro-electronic cooling systems.

Key words: *oblique finned micro-channel, CFD, nanofluid, heat transfer rate, trapezoidal cross-section*

Introduction

The drift towards the miniaturization and advancement in micro-technology leads to the development of micro-channel to remove the high heat fluxes from the electronic devices. The various fields include space technology, electronics, military, and very large scale integrated cooling systems. The heat removal in electronics chips was found to be challenging, and there is more research being carried out in dissipating heat using micro-channel heat sink [1].

Many of the micro-channel design has been modified and studied, to achieve the higher heat transfer rate [2-5]. Ramos-Alvarado *et al*. [2] carried a CFD study and heat transfer performance of the liquid cooled heat sinks. They analyzed flow distribution using the CFD software ANSYS FLUENT. The results of this study show the basic concept of flow distributor with symmetric flow bifurcations, as demonstrated in the Distributor-A and B configurations are highly recommended. Mushtaq *et al*. [3] performed heat transfer analysis in various cross-sections such as square, rectangular, iso-triangular, and trapezoidal. They predicted a new co-relation in a heat exchanger to enhance the heat transfer performance. Qu *et al*. [4] conducted experiments to investigate the flow characteristics through trapezoidal channel. They found that the friction flow and pressure gradient were higher than the conventional laminar flow theory. Kuppusamy

* Corresponding author, e-mail: rvinomech@gmail.com

et al. [5] enhanced the heat transfer performance in trapezoidal channels. The increase in maximum width and the decrease in minimum depth for the trapezoidal channel will improve the heat transfer performance.

The nanofluids can be used in the micro-channel heat sink for further useful heat transfer rate enhancement. Several types of research have been carried out on nanofluid as a coolant in micro-channel [6-12]. Yang *et al*. [6] executed the numerical study of flow and heat transfer characteristics of Al_2O_3-water nanofluids in a micro-channel. The simulation was conducted at low Reynolds number ($Re \leq 16$) using lattice Boltzmann method (LBM). They observed that the fluid temperature distribution was more uniform with the use of nanofluid than that of pure water. Selvakumar and Suresh [7] did a study on the effect of CuO-water nanofluids in a thin copper channel heat sink under constant heat flux condition with volume fractions 0.1% and 0.2%. As a result, the maximum increase in convective heat transfer coefficient determined as 29.63% for the nanofluid having a volume fraction of 0.2% compared to deionized water for the same volume flow rate. Ebrahimnia-Bajestan [8] investigated the heat transfer performance and pressure drop in straight circular pipe numerically. The $A1_2O_3$, CuO, carbon nanotube (CNT), and titanate nanotube (TNT) nanoparticles were used as working fluids. The outcome of the study is that nanoparticle and base fluid influence heat transfer performance of nanofluids. Dorin [9] performed the evaluation of Al_2O_3-water nanofluid in the micro-channel heat sink. The heat sink with square micro-channels and $D_h = 50$ μm was assigned. The water-based Al_2O_3 nanofluid was used as the working fluid with various volume concentrations.The performance evaluation showed that heat transfer decreases as the particle diameter increases. Chang *et al*. [10] conducted an investigation on the effects of the particle volume fraction on the spray. The nanofluid containing de-ionized water and Al_2O_3 particles were used as the test fluid. They obtained the optimal heat transfer using a particle volume fraction of 0.001%. Shalchi-Tabrizi and Seyf [11] numerically analyzed the entropy generation and convective heat transfer of $A1_2O_3$ nanofluid in a tangential micro-channel heat sink. The results indicated that the generated total entropy decreases with the increase of volume fraction and Reynolds number and thereby decreasing the particle size. Kalteh *et al*. [12] studied the convective heat transfer of Al_2O_3 nanofluid in a rectangular heat sink. The finite volume approach was adopted using the Eulerian-Eulerian method. They concluded that Nusselt number increases with the increase in Reynolds number.

It was found from the literature survey, heat transfer performance of micro-channel heat sink is increased by changing design and coolant. This work deals with heat transfer study in the oblique finned micro-channel for different inlet cross-sections. The coolants are water and Al_2O_3-water nanofluid with 0.25% volume fraction was used as heat transfer fluids. In which the three different inlet cross-sections namely trapezoidal, square and semicircle are also compared. By varying the Reynolds number, the heat transfer characteristics and flow characteristics are studied numerically. The ANSYS FLUENT simulation was validated with existing experimental works. The analysis results of three cross-sections are compared with each other, and the desired performance is finally accomplished.

Materials and methods

Micro-channel geometry

The micro-channel heat sink is containing an array of 775 oblique fins with three different inlet cross-sections. The material was taken as Cu with the dimensions of 48×80 mm and designed with CATIA. Figure 1(a) shows the design of oblique finned micro-channel with multiple parallel channels. Figure 1(b) shows the different inlet cross-sections of square, semi-circular and trapezoidal channels were used for the study.

The micro-channel contains three cross-sections for the overlook. The dimensions are given in tab. 1.

Thermo-physical properties of working fluid

From theoretical studies on particle-fluid mixtures, the properties of nanofluids can be determined by the following formula.

Pang *et al*. [13] measured the thermal conductivity of nanofluids. The formula to find the thermal conductivity of nanofluid is:

$$k_{\mathrm{nf}} = \frac{k_{\mathrm{p}} + 2k_{\mathrm{bf}} + 2\left(k_{\mathrm{p}} - k_{\mathrm{bf}}\right)\varphi}{k_{\mathrm{p}} + 2k_{\mathrm{bf}} - 2\left(k_{\mathrm{p}} - k_{\mathrm{bf}}\right)\varphi} \quad (1)$$

Solve by governing equation $C_{p,\mathrm{nf}}$, Hung *et al*. [14] proposed the heat capacity equation, which is:

$$C_{p,\mathrm{nf}} = \frac{(1-\varphi)\left(\rho C_p\right)_{\mathrm{bf}} + \varphi\left(\rho C_p\right)_{\mathrm{p}}}{\rho_{\mathrm{nf}}} \quad (2)$$

The density of the nanofluid is calculated by according to Mohammed *et al*. [15].

$$\rho_{\mathrm{nf}} = (1-\varphi)\rho_{\mathrm{bf}} + \varphi\rho_{\mathrm{p}} \quad (3)$$

Theoretical investigations on the viscosity of nanofluid are given by Mahbubul *et al*. [16] in the latest development of viscosity in a nanofluid. They concluded that particle size had adverse effects on nanofluid:

$$\mu_{\mathrm{nf}} = \mu_{\mathrm{bf}}\left(1 + 2.5\varphi\right) \quad (4)$$

where suffix *bf* represents base fluids, and *nf* represents nanoparticles. The properties of nanofluids are summarized in tab. 2.

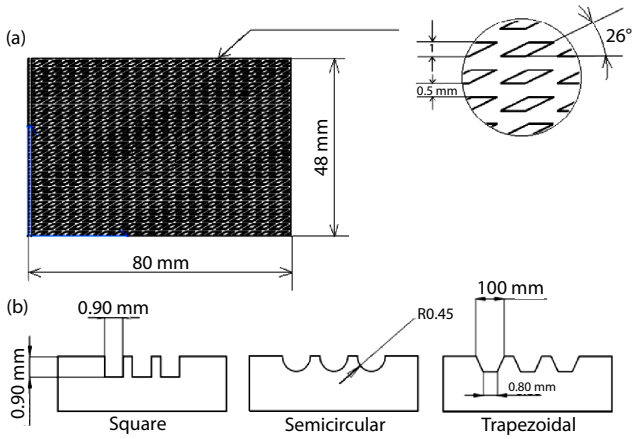

Figure 1. (a) Oblique finned micro-channel, (b) different inlet cross-sections of the oblique finned micro-channel

Table 1. The dimensions of the oblique finned micro-channel with three inlet cross-sections

Characteristic	Semicircular	Square	Trapezoidal
Footprint, width × length [mm]	48 × 80	48 × 80	48 × 80
Main channel width, W_c [μm]	900	900	900
Fin width, W_w [μm]	800	800	900
Channel depth, H [μm]	800	800	800
Fin length, L [μm]	1000	1000	1000
Fin pitch, P [μm]	800	800	800
Oblique angle, θ, [°]	26	26	26

Table 2. Properties of nanofluid (Al_2O_3)

Fluids	Concentration, φ [%]	Thermal conductivity, k [$Wm^{-1}K^{-1}$]	Specific heat capacity, C_p [$Jkg^{-1}K^{-1}$]	Density, ρ [kgm^{-3}]	Viscosity, μ, $\times 10^{-3}$ [Nsm^{-2}]
Aluminum oxide	0.25	1.0071	4163.83	1008	0.8440

Computational model

Boundary conditions

The heat sink covered by a thermally insulating material and therefore the boundary of the top surface is assumed to be adiabatic. The inner surface of the wall and the micro-channel are considered as adiabatic. In the fluid region, uniform velocity and temperature are applied at the inlet of the micro-channel. At the exit of the micro-channel, the coolant is assumed to have an equal pressure to determine the pressure drop. The boundary condition for numerical analysis is taken based on data collection for various studies are:

Inlet temperature = 293.2 K Inlet pressure = 1 bar

Reynolds number = 99, 197, 296, 395, 494 Constant heat flux = 20000 W/m^2

The inlet velocity is taken based on the Reynolds number of the fluids. Constant heat flux is supplied to the base of the micro-channel for both water and nanofluid. The numerical work employed to perform this study is carried out by ANSYS FLUENT. The heat transfer analysis is carried out in steady-state single phase flow and determining the temperature and pressure distribution.

Grid independent test

The algorithm that diverges extremely little as the cell size is increased. The variation of the predicted temperature and pressure with distance is plotted in figs. 2(a) and 2(b). There are four types of quadrilateral meshes with grid lines of 94 × 68 × 56, 98 × 70 × 62, 102 × 72 × 68, and 108 × 78 × 72 are investigated for square geometrical configuration. The temperature and pressure vary between 293.2 to 298.1 K and 101.31 to 101.59 kPa. The difference in the temperature and pressure between mesh 94 × 68 × 56 and mesh 98 × 70 × 62 is 0.69%, and mesh 98 × 70 × 62 and mesh 102 × 72 × 68 is 0.6%. The temperature and pressure are negligible from the mesh 102 × 72 × 68 to mesh 108 × 78 × 72 that is the percentage deviation of only 0.1%. Finally, the 102 × 72 × 68 grid was selected as the best trade-off between both accuracy and CPU time.

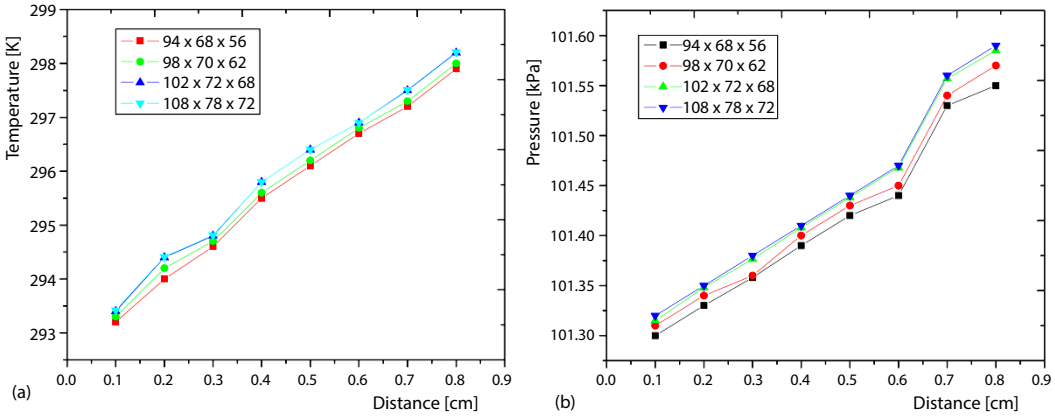

Figure 2. Comparison of streamwise temperature distribution; (a) and pressure distribution (b) with various meshing count

Data reduction

Heat transfer rate and average Nusselt number are calculated:

– the minimum flow area in the channel is obtained by Siddiqui *et al.* [17]:

$$A_{\min} = W_c H \frac{\frac{W_c}{\sin\theta}}{2S_T} \tag{5}$$

– the heat transferred by the micro-channel can be calculated from inlet and outlet temperatures. The heat transfer equation is given by Yu *et al*. [18]:

$$Q = \dot{m} C_p (T_{\text{out}} - T_{\text{in}}) \tag{6}$$

where C_p is the specific heat capacity.

– the average Nusselt number is worked out using the following equation given by Ganapathy *et al*. [19]:

$$\text{Nu} = \frac{hD_h}{k} \tag{7}$$

where D_h is the micro-channel hydraulic diameter and k – the thermal conductivity of the fluid.

– the heat transfer coefficient is worked out using the following relation, which is given by Dede and Liu [20]:

$$h = \frac{q}{T_s - \frac{T_{\text{in}} - T_{\text{out}}}{2}} \tag{8}$$

where T_s is the surface temperature, and q – the constant heat flux supplied during the heat transfer analysis.

– the pressure drop calculated from the work of Pandey and Nema [21]:

$$\Delta p = p_{\text{in}} - p_{\text{out}} \tag{9}$$

where p_{in} refers to the pressure at the inlet of the micro-channel and p_{out} – the pressure at the outlet of the micro-channel.

– the friction factor was calculated from the work of Fan *et al*. [22]:

$$f = \frac{D_h}{4L} \frac{\Delta p}{0.5\rho u^2} \tag{10}$$

where ρ is fluid density and u is average fluid velocity.

Numerical study

The oblique fined micro-channel had been designed for three inlet cross-sections namely, square, semicircle, and trapezoidal. Temperature distributions and pressure distribution along the length of the channels are tested for Reynolds number ranging between 99 and 494. Water and nanofluid are examined for temperature and pressure variation along the channel length.

Temperature and pressure variation for trapezoidal cross-section

The pressure distribution and the temperature distribution of the water and nanofluid in the trapezoidal cross-section are analyzed in figs. 3(a) and 3(b), where the fluid exits the micro-channel at 299.74 K and 296.96 K for nanofluid and water, respectively. In the case of pressure, the inlet pressure is 102113.8 Pa and 101591.97 Pa for water and nanofluid, respectively.

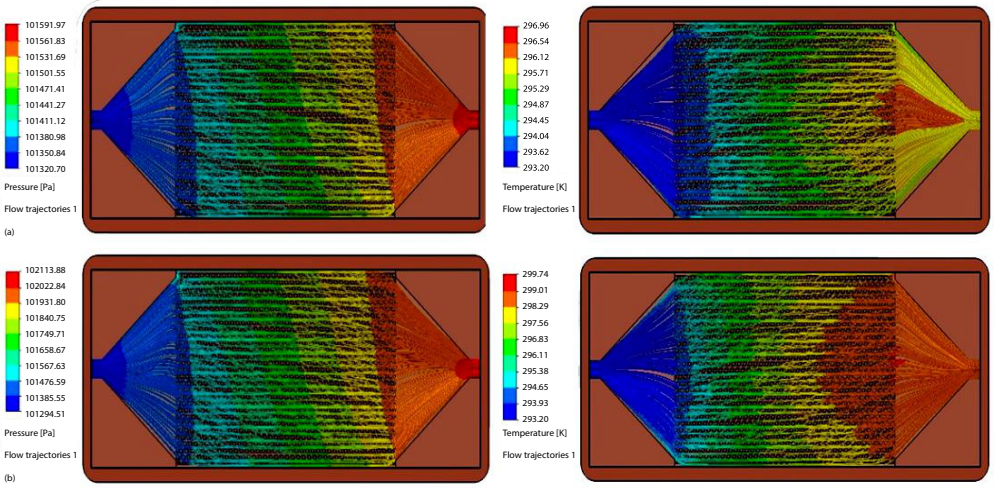

Figure 3(a) and 3(b). Pressure and temperature distribution in trapezoidal microchannel using nanofluid and water (*for color image see journal web site*)

In fig. 3(a), the pressure drop is 819.37 Pa occurs due to the flow of the nanofluid in the trapezoidal cross-section micro-channel heat sink. From the figure, it can also be observed that the temperature rises to 299.74 K at the exit of the nanofluid. The pressure and temperature distribution are obtained for the 0.1 kg/min of mass-flow rate which can similarly be obtained for the other mass-flow rates of nanofluid. In fig. 3(b), the pressure and temperature distributions for the water in 0.1 kg/min of mass-flow rate of water are shown. The amount of pressure drop and temperature rise is 271.27 Pa and 3.96 K. The pressure drop is high due to the absence of nanoparticles creating ease of flow, and the temperature variance is due to the increase in the overall heat transfer coefficient. The heat transfer coefficient is increased due to the presence of the nanoparticles.

Temperature and pressure variation for square cross-section

The square cross-section micro-channel is analyzed for the pressure and temperature with the flow of the water and nanofluid as shown in figs. 4(a) and 4(b). The pressure variations from 101486.65 Pa to 101320.03 Pa in the case of the square cross-section with nanofluid as the coolant reveal in fig. 4(a) and also the temperature drops from 299.71-293.2 K. From the fig. 4 (b) it can be observed that the pressure decreases from 101751.2-101291.94 Pa on using water.

The temperature rise is of 3.56 K which is the difference of 296.76 k and 293.2 K. The distribution is obtained for the 0.1 kg/min of mass-flow rate of water which can also be obtained for the other mass-flow rate. The reason lies the same as the trapezoidal for the temperature rise and pressure drop for the square cross-section also.

Temperature and pressure variation for semicircle cross-section

The pressure and temperature distribution of the water and nanofluid are studied in semicircle cross-section as shown in figs. 5(a) and 5(b). The pressure drop is 254.23 Pa in the case of nanofluid which is observed in fig. 5(a) also the temperature distributions vary from 299.64 to 293.2 K. In fig. 5(b) shows the pressure and the temperature distribution of water. The pressure drop and temperature differences are 254 Pa and 3.57 K, respectively.

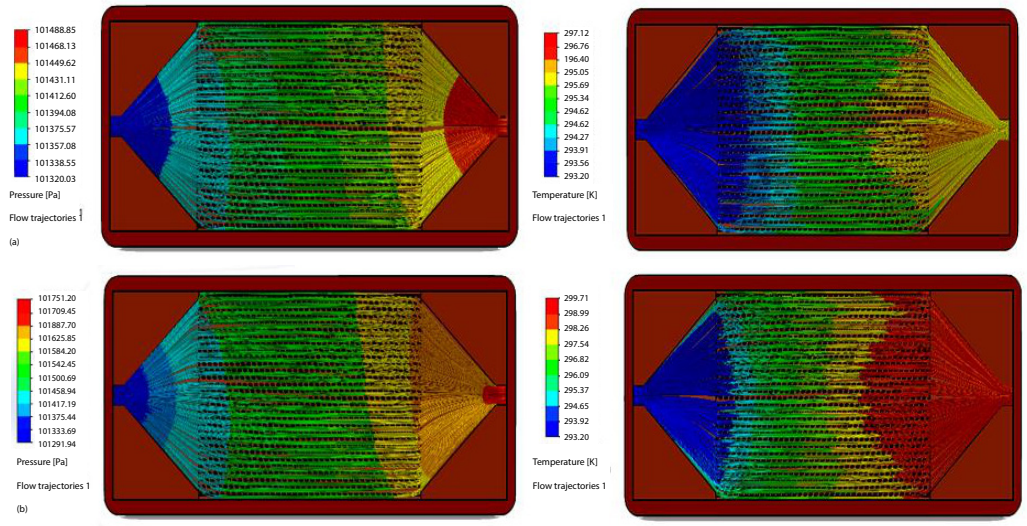

Figure 4(a) and 4(b). Representation of pressure and temperature over the square cross-section using nanofluid and water (*for color image see journal web site*)

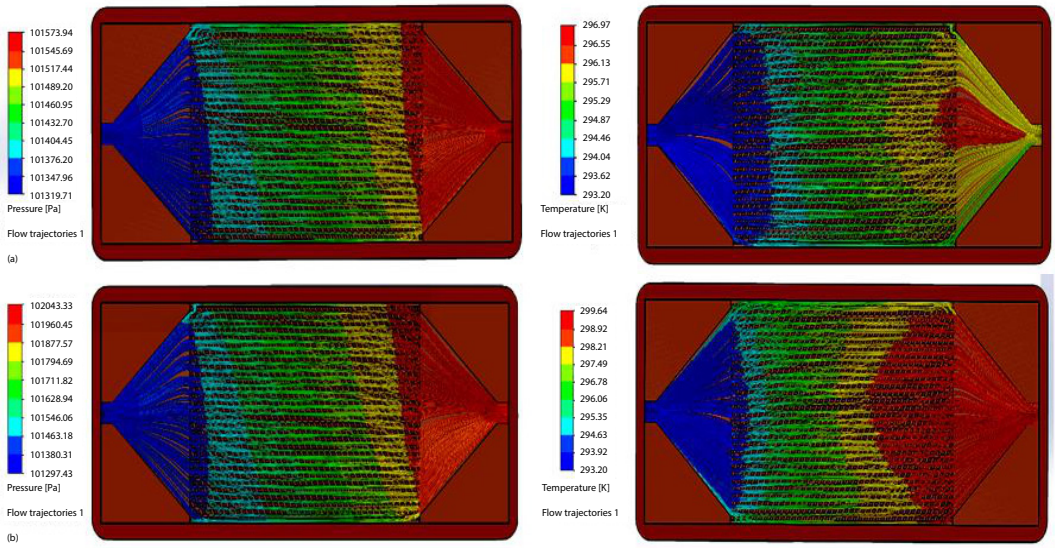

Figure 5(a) and 5(b). Semicircle cross-section pressure and temperature distribution using nanofluid and water (*for color image see journal web site*)

This temperature rise and the pressure drop is less when compared to that of the trapezoidal cross-section.

Results and discussion

Validation of numerical simulation

Before conducting the numerical study, it is necessary to validate the numerical simulation by comparing with the existing experimental work. The width of the micro-channel is 700 μm,

the height of the micro-channel is 700 µm, and the length is 80 mm which are all the same in numerical work. The working fluid used for validation is water with a square cross-section. The current numerical work was carried out by using the same dimension as per existing experimental work, and the Nusselt number is calculated by using the correlation. Thus the Reynolds number and Nusselt number values were compared with existing experimental work.

The ANSYS FLUENT simulation is validated with the aid of an existing experimental work of Fan *et al*. [22], Kalteh *et al*. [12], and Chai *et al*. [23]. Figure 6 shows the comparison of the present simulated work and previous experimental work. The data matched quite well with the numerical simulation with the acceptable deviation of 5.9%. This deviation may be due to an error in the heat loss. It shows that there is a good agreement between existing experimental work and simulation. The Nusselt number was found to be 5.1 to 8.6 by variation of Reynolds number from 99 to 494.

Outlet temperature variation

From the numerical results, the outlet temperature was measured for the three cross--sections using water and nanofluid and studied by varying the Reynolds number. In fig. 7, the outlet temperature is plotted against the Reynolds number where the temperature falls as the velocity increases. It is observed that the trapezoidal cross-section values are higher than the square and semicircle. Moreover, also it can be seen that nanofluid also influences the outlet temperature of the working fluid absorbed more heat from the micro-channel than the water. This is due to the addition of the nanoparticles.

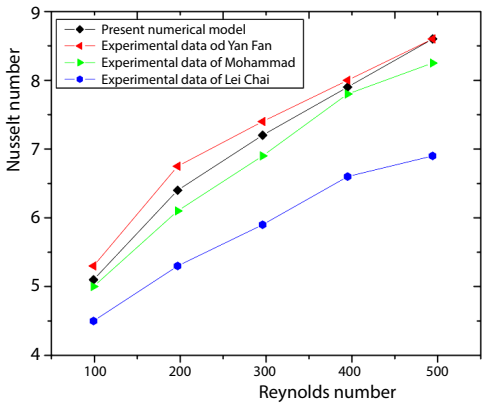

Figure 6. Comparison of the numerical simulation with experimental work

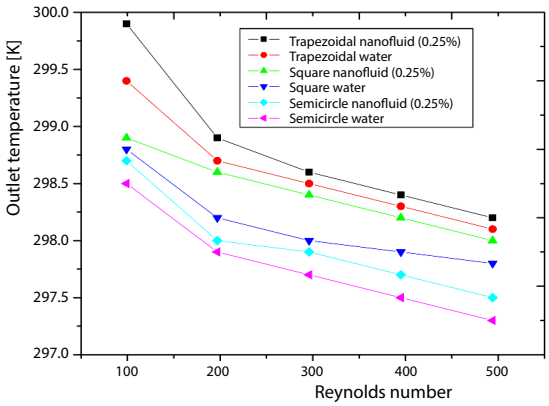

Figure 7. Outlet temperature with Reynolds number for three cross-sections with water and nanofluid

Nusselt number and heat transfer rate characteristic

Heat transfer rate and Nusselt number are compared for the three different inlet cross-section using water and nanofluids. The heat transfer performance of the micro-channel heat sink is plotted figs. 8(a) and 8(b). The average nusselt number increase with Reynolds number as the thermal boundary-layer thickness decreases with increase in fluid velocity. Reynolds number increases with the increase in Nusselt number for both nanofluid and water. Nanofluid with Al_2O_3 0.25% is having the higher Nusselt number of 16.38 at Re = 494. The Nusselt number of nanofluid is greater than water by 0.5. The divergence of the water and nanofluid was 3.388% in case of trapezoidal. For Reynolds number ranging between 99 and 494,

the heat transfer rate increases from 11.34 to 18.8 W for nanofluid with 0.25% concentration. The percentage deviation is about 8.66% of the water and nanofluid in the case of trapezoidal cross-section. The heat transfer rate is more in the case of the trapezoidal cross-section for both water and nanofluid.

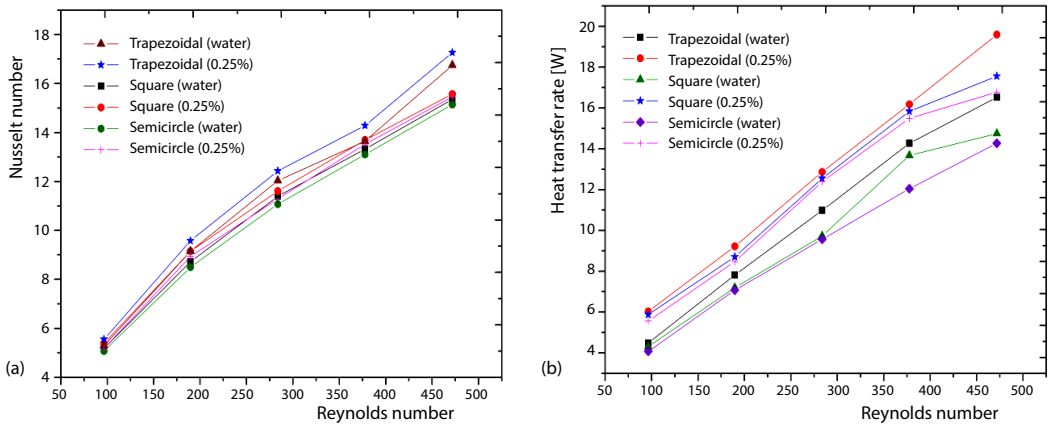

Figure 8(a) and 8(b). Variation of the Nusselt number and heat transfer rate with water and nanofluid for the different cross-section

The significant heat transfer enhancement in the trapezoidal cross-section is due to larger wall area and effective entrance length. Also, the trapezoidal cross-section has more influence in secondary flow due to the shape of the oblique fin and minimum thermal resistance, this causes an increase in heat transfer rate.

Pressure drop and friction factor characteristics

Pressure drop and friction factor are found for the three inlet cross-section for the comparison study, which is plotted in the figs. 9(a) and 9(b).

In fig. 9(a) shows the Reynolds number increases with the increase in pressure drop [kPa] for both fluids. The pressure drops higher for nanofluid due to higher viscosity. Nanofluid with Al_2O_3 0.25% is having the greater pressure drop of 3.6 kPa at Re = 494. Consistently the

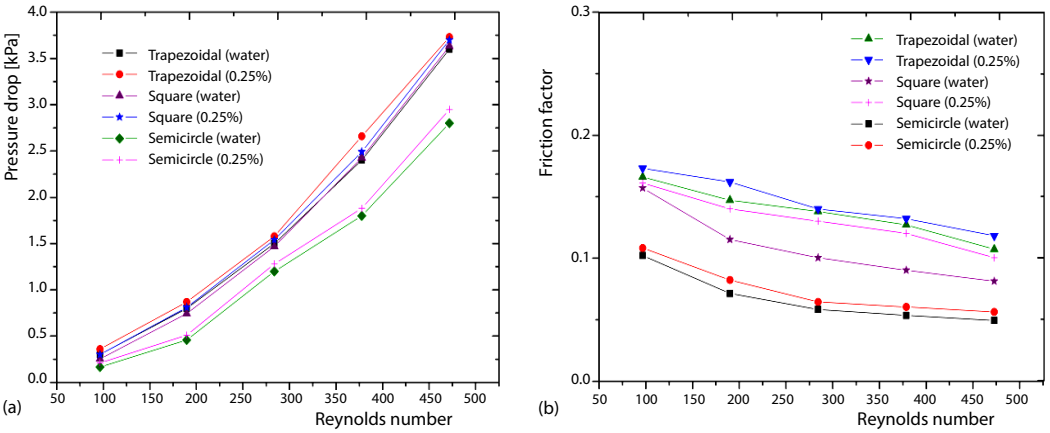

Figure 9(a) and 9(b). Effect of pressure drop and friction factor with water and nanofluid for the different cross-section

trapezoidal cross-section is producing higher values. The difference between the values of water and nanofluid in the trapezoidal cross-section is 8.6%. The variation clearly denotes the flow to be laminar, and the friction factor decreases with an increase with an increase in Reynolds number as shown in fig. 9(b). It is clear that trapezoidal cross-section has higher values of friction factor than that of the other two cross-sections with both water and nanofluid (0.25%). The percentage deviation between the water and nanofluid in the trapezoidal cross-section was found to be 5.5%. The friction factor is high in case of trapezoidal cross-section due to the larger section of size wall, which is directly responsible for the pressure drop. The addition of nanoparticles with base fluid increases the thermal performance. There is a drawback associated with an increase of the pressure drop in the device with an increase in volume fraction of nanofluid.

Conclusions

Numerical study of the heat transfer and flow characteristics on the micro-channel heat sink was investigated by flowing water and nanofluid (0.25%) as a coolant. The results are compared for three different cross-sections by varying the Reynolds number. The following conclusions were drawn.

- The heat transfer rate of three cross-sections have been compared, and trapezoidal is found to be the better one with deviations of 5.7% and 9.8% with square and semicircle, respectively, and also the Nusselt number augmented by the trapezoidal cross-section.
- The addition of nanoparticles to the base fluid increases the heat transfer rate by 3.38 % than the water for the trapezoidal cross-section.
- Pressure drop also had a considerable raise in its magnitude in trapezoidal cross-section which also influenced the friction factor. The nanofluid has an enhanced pressure drop of 8.6% over water. Also, there is 5.5 % raise in friction factor when nanofluid is used in the trapezoidal cross-section.
- Eventually, the trapezoidal cross-section is found to achieve superior in heat transfer and flow characteristics when compared with square and semicircle cross-section profile.

Nomenclature

C_p – specific heat, [Jkg^{-1}K^{-1}]
D_h – hydraulic diameter, [µm]
f – friction factor
H – channel depth, [µm]
h – heat transfer coefficient, [Wm^{-2}K^{-1}]
k – thermal conductivity, [Wm^{-1}K^{-1}]
L – length, [m]
$\dot{m}$ – mass-flow rate, [kgs^{-1}]
Nu – Nusselt number
P – fin pitch, [µm]
p – pressure
Δp – pressure drop
Q – heat transfer co-efficient, [Wm^{-2}K^{-1}]
Re – Reynolds number
S_T – transverse pitch, [mm]
T – temperature, [K]
T_s – surface temperature
u – velocity, [ms^{-1}]
W_c – channel width, [µm]
W_w – fin width, [µm]

Subscripts

bf – basefluid
h – hydraulic
in – inlet
nf – nanofluid
out – outlet
p – particle
s – surface

Greek symbols

θ – oblique angle, [°]
μ – viscosity, [Nsm^{-2}]
ρ – density, [kgm^{-3}]
φ – volume concentration, [%]

References

[1] Shanglong, X. U., *et al*., Optimization of theThermal Performance of Multi-Layer Silicon Microchannel Heat Sinks, *Thermal Science*, *20* (2016), 6, pp. 2001-2013

[2] Ramos-Alvarado, B., *et al.,* CFD Study of Liquid-Cooled Heat Sinks with Microchannel Flow Field Configurations for Electronics, Fuel Cells, and Concentrated Solar Cells, *Applied Thermal Engineering*, *31* (2011), 14-15, pp. 2494-2507
[3] Mushtaq, I. H., *et al*., Influence of Channel Geometry on the Performance of a Counter Flow Microchannel Heat Exchanger, *International Journal of Thermal Sciences*, *48* (2009), 8, pp.1607-1618
[4] Qu, W., *et al*., Pressure-Driven Water Flows in Trapezoidal Silicon Microchannels, *International Journal of Heat and Mass Transfer*, *43* (2000), 3, pp. 353-364
[5] Kuppusamy, N. R., *et al*., Numerical Investigation of Trapezoidal Grooved Microchannel Heat Sink Using Nanofluids, *Thermochimica Acta*, *573* (2013), Dec., pp. 39-56
[6] Yang, Y.-T., *et al*., Numerical Study of Microchannel Heat Sink Performance Using Nanofluids, *International Communications in Heat and Mass Transfer*, *57* (2014), Oct., pp. 27-35
[7] Selvakumar, P., Suresh, S., Convective Performance of CuO/Water Nanofluid in an Electronic Heat Sink, *Experimental Thermal and Fluid Science*, *40* (2012), July, pp. 57-63
[8] Ebrahimnia-Bajestan., E., *et al*., Numerical Investigation of Effective Parameters in Convective Heat Transfer of Nanofluids Flowing under a Laminar Flow Regime, *International Journal of Heat and Mass Transfer*, *54* (2011), 19-20, pp. 4376-4388
[9] Dorin, L., The Performance Evaluation of Al_2O_3/Water Nanofluid Flow and Heat Transfer Microchannel Heat Sink, *International Journal of Heat and Mass Transfer*, *54* (2011), 17-18, pp. 3891-3899
[10] Chang, T.-B., *et al*., Effects of Particle Volume Fraction on Spray Heat Transfer Performance of Al_2O_3/Water Nanofluid, *International Journal of Heat and Mass Transfer*, *55* (2012), 4, pp. 1014-1021
[11] Shalchi-Tabrizi, A., Seyf, H. R., Analysis of Entropy Generation and Convective Heat Transfer of Al_2O_3 Nanofluid Flow in a Tangential Micro Heat Sink, *International Journal of Heat and Mass Transfer*, *55* (2012), 15-16, pp. 4366-4375
[12] Kalteh., M., *et al*., Experimental and Numerical Investigation of Nanofluid Forced Convection inside a Wide Micro Channel Heat Sink, *Applied Thermal Engineering*, *36* (2012), 1, pp. 260-268
[13] Pang, C., *et al*., Thermal Conductivity Measurement of Methanol-Based Nanofluids with Al_2O_3 and SiO_2 Nanoparticles, *International Journal of Heat and Mass Transfer*, *55* (2012), 21-22, pp. 5597-5602
[14] Hung, T.-C., *et al*., Heat Transfer Enhancement in Microchannel Heat Sinks Using Nanofluids, *International Journal of Heat and Mass Transfer*, *55* (2012), 9-10, pp. 2559-2570
[15] Mohammed, H. A., *et al*., Influence of Various Base Nanofluids and Substrate Materials on Heat Transfer in Trapezoidal Microchannel Heat Sinks, *International Communications in Heat and Mass Transfer*, *38* (2011), 2, pp. 194-201
[16] Mahbubul, I. M., *et al*., Latest Developments on the Viscosity of Nanofluids, *International Journal of Heat and Mass Transfer*, *55* (2012), 4, pp. 874-885
[17] Siddiqui, F. A., *et al*., Experimental Investigation of Air Side Heat Transfer and Fluid Flow Performances of Multi-Port Serpentine Cross-Flow Microchannel Heat Exchanger, *International Journal of Heat and Fluid Flow*, *33* (2012), 1, pp. 207-219
[18] Yu, X.-F., *et al*., A Study on the Hydraulic and Thermal Characteristics in Fractal Tree-Like Microchannels by Numerical and Experimental Methods, *International Journal of Heat and Mass Transfer*, *55* (2012), 25-26, pp. 7499-7507
[19] Ganapathy, H., *et al*., Volume of Fluid-Based Numerical Modeling of Condensation Heat Transfer and Fluid Flow Characteristics in Microchannels, *International Journal of Heat and Mass Transfer*, *65* (2013), Oct., pp. 62-72
[20] Dede, E. M., Liu, Y., Experimental and Numerical Investigation of a Multi-Pass Branching Microchannel Heat Sink, *Applied Thermal Engineering*, *55* (2013), 1-2, pp. 51-60
[21] Pandey, S. D., Nema, V. K., Experimental Analysis of Heat Transfer and Friction Factor of Nanofluid as a Coolant in a Corrugated Plate Heat Exchanger, *Experimental Thermal and Fluid Science*, *38* (2012), Apr., pp. 248-256
[22] Fan, Y., *et al*., A Simulation and Experimental Study of Fluid Flow and Heat Transfer on Cylindrical Oblique-Finned Heat Sink, *International Journal of Heat and Mass Transfer, 61* (2013), June, pp. 62-72
[23] Chai, L., *et al*., Parametric Study on Thermal and Hydraulic Characteristics of Laminar Flow in Microchannel Heat Sink with Fan-Shaped Ribs on Sidewalls, *International Journal of Heat and Mass Transfer*, *97* (2016), June, pp. 1069-1080

Paper submitted: November 19, 2016
Paper revised: May 23, 2017
Paper accepted: May 28, 2017